

hp-Adaptive Discontinuous Galerkin Methods for Porous Media Flow

Birane Kane, Robert Klöfkor and Christoph Gersbacher

Abstract We present an adaptive Discontinuous Galerkin discretization for the solution of porous media flow problems. The considered flows are immiscible and incompressible. The adaptive approach implemented allows for refinement/coarsening in both the element size and the polynomial degree. The method is evaluated using homogeneous and heterogeneous test cases.

Keywords *hp*-Adaptivity · Fully implicit · Discontinuous galerkin · DUNE

MSC (2010): 65M08 · 65M60 · 65M50

1 Introduction

The modeling and simulation of flow in porous media is essential in many environmental problems such as groundwater flow and petroleum engineering. The inherent geological complexity and the strong heterogeneity of the soil parameters require locally conservative methods such as Discontinuous Galerkin (DG) methods in order to be able to follow small concentrations [1].

The first *h*-adaptive DG framework for porous media two-phase flow was introduced by Klieber and Rivi re [11]. The authors used a decoupled formulation with continuous capillary pressure functions, only $2d$ flow on non-conforming simplicial grids were considered and they implemented an error indicator obtained from

B. Kane

University of Stuttgart, Stuttgart, Germany
e-mail: birane.kane@ians.uni-stuttgart.de

R. Kl fkor (✉)

International Research Institute of Stavanger, Stavanger, Norway
e-mail: robert.kloefkor@iris.no

C. Gersbacher

University of Freiburg, Freiburg, Germany
e-mail: gersbach@mathematik.uni-freiburg.de

  Springer International Publishing AG 2017

C. Canc s and P. Omnes (eds.), *Finite Volumes for Complex Applications VIII—Hyperbolic, Elliptic and Parabolic Problems*, Springer Proceedings in Mathematics & Statistics 200, DOI 10.1007/978-3-319-57394-6_47

transient linear convection diffusion problems [9]. More recently, Kane [10] implemented a higher order h -adaptive scheme for $2d$ and $3d$ two-phase flow problem with strong heterogeneity, discontinuous capillary pressure functions and gravity effects. The results in [10] show that an increase of the polynomial degree gives a considerable improvement of the solution with sharper fronts and the oscillations appearing in the vicinity of the front are reduced with the local mesh refinement. A discretization scheme independent abstract framework allowing for a more rigorous a-posteriori estimator for porous media two-phase flow problem was introduced by [13]. This paved the way for a h -adaptive strategy for a homogeneous two-phase flow problem. However it has only been applied so far to Finite Volume methods [6].

The first contribution of this work is to provide a first and second order Adam-Moulton time discretization combined with the Interior Penalty DG methods. This implicit space time discretization leads to a fully coupled nonlinear system requiring to build a Jacobian matrix at each time step for the Newton-Raphson method. The second contribution of this work is providing a hp -adaptive strategy extending the previous work of [10], this is the first porous media two-phase flow fully adaptive scheme allowing for adaptivity for both the element size and the polynomial degree. This hp -adaptive strategy allows to refine the mesh when the solution is estimated to be rough and increase the polynomial degree when the solution is estimated to be smooth hence compensating the increased computational cost for complex models.

The rest of this document is organised as follows. In the next section, we describe the two-phase flow model. The DG discretization is introduced in Sect. 3. The adaptive strategy in space is outlined in Sect. 4. Numerical examples are provided in Sect. 5. Finally concluding remarks are provided in the last section.

2 Governing Equations

We consider an open and bounded domain $\Omega \in \mathbb{R}^d$, $d \in \{1, 2, 3\}$ and the time interval $\mathcal{J} = (0, T)$, $T > 0$. The flow of the wetting-phase and the nonwetting-phase is described by the Darcy's law and the continuity equation for each phase, namely, with $\sum_{\alpha} s_{\alpha} = 1$ and $p_n - p_w = p_c(s_{w,e})$,

$$v_{\alpha} = -\lambda_{\alpha} K (\nabla p_{\alpha} - \rho_{\alpha} g) \text{ and } \phi \frac{\partial \rho_{\alpha} s_{\alpha}}{\partial t} + \nabla \cdot (\rho_{\alpha} v_{\alpha}) = \rho_{\alpha} q_{\alpha}. \quad (1)$$

Here, we search for the phase pressures p_{α} and the phase saturations s_{α} , $\alpha \in \{w, n\}$. We denote with subscript w the wetting-phase and with subscript n the nonwetting-phase. K is the permeability of the porous medium, ρ_{α} is the phase density, q_{α} is a source/sink term and g is the constant gravitational vector. We assume the porosity ϕ is time independent and there exist $\phi_1, \phi_2 > 0$ such that $0 < \phi_1 \leq \phi \leq \phi_2$ and with the phase mobilities $\lambda_{\alpha} = \frac{k_{r\alpha}}{\mu_{\alpha}}$, $\alpha \in \{w, n\}$, where μ_{α} is the phase viscosity and

$k_{r\alpha}$ is the relative permeability of phase α . The relative permeabilities are functions that depend on the phase saturation in nonlinear fashion (i.e. $k_{r\alpha} = k_{r\alpha}(s_\alpha)$). For example, in the Brooks-Corey model [5], $k_{rw}(s_{w,e}) = s_{w,e}^{\frac{2+3\theta}{\theta}}$, $k_{rn}(s_{n,e}) = (s_{n,e})^2(1 - (1 - s_{n,e})^{\frac{2+\theta}{\theta}})$, where the effective saturation $s_{\alpha,e}$ is $s_{\alpha,e} = \frac{s_\alpha - s_{\alpha,r}}{1 - s_{w,r} - s_{n,r}}$, $\forall \alpha \in \{w, n\}$. Here, $s_{\alpha,r}$, $\alpha \in \{w, n\}$ are the phase residual saturations. The parameter $\theta \in [0.2, 3.0]$ is a result of the inhomogeneity of the medium. The capillary pressure $p_c = p_c(s_{w,e})$ is a function of the phase saturation $p_c(s_{w,e}) = p_d s_{w,e}^{-1/\theta}$ where $p_d \geq 0$ is the constant entry pressure.

From the constitutive relations $s_w + s_n = 1$ and $p_n - p_w = p_c(s_{w,e})$, we can rewrite the two-phase flow problem as a system of equations with two unknowns p_w and s_n ,

$$\begin{aligned}
 -\nabla \cdot (\lambda_t K \nabla p_w + \lambda_n K \nabla p_c - (\rho_w \lambda_w + \rho_n \lambda_n) K g) &= q_w + q_n, \\
 \phi \frac{\partial s_n}{\partial t} - \nabla \cdot (\lambda_n K (\nabla p_w - \rho_n g)) - \nabla \cdot (\lambda_n K \nabla p_c) &= q_n.
 \end{aligned}
 \tag{2}$$

Here, $\lambda_t = \lambda_w + \lambda_n$ denotes the total mobility.

The first equation of (2) is of elliptic type with respect to the pressure p_w . The type of the second equation of (2) is either nonlinear hyperbolic if $\frac{\partial p_c(s_n)}{\partial s_n} \equiv 0$ or degenerate parabolic if the capillary pressure is not neglected. The diffusion term might degenerate if $\lambda_n(s_n = 0) = 0$. In order to have a complete system we add appropriate boundary and initial conditions. Thus, we assume that the boundary of the system is divided into disjoint open sets $\partial\Omega = \bar{\Gamma}_D \cup \bar{\Gamma}_N$. We define the total inflow $J_t = J_w + J_n$ as the sum of the phases inflow on the Neumann boundary $\bar{\Gamma}_N$.

3 Discretization

Let $\mathcal{T}_h = \{E\}$ be a family of non-degenerate, quasi-uniform, possibly non-conforming partitions of Ω consisting of N_h elements (quadrilaterals or triangles in 2d, tetrahedrons or hexahedrons in 3d) of maximum diameter h . Let Γ^h be the union of the open sets that coincide with internal interfaces of elements of \mathcal{T}_h . Dirichlet and Neumann boundary interfaces are collected in the set Γ_D^h and Γ_N^h . Let e denote an interface in Γ^h shared by two elements E_- and E_+ of \mathcal{T}_h ; we associate with e a unit normal vector n_e directed from E_- to E_+ . We also denote by $|e|$ the measure of e . The discontinuous finite element space is $\mathcal{D}_r(\mathcal{T}_h) = \{v \in \mathbb{L}^2(\Omega) : v|_E \in \mathcal{P}_r(E) \ \forall E \in \mathcal{T}_h\}$, where $\mathcal{P}_r(E)$ denotes \mathbb{Q}_r (resp. \mathbb{P}_r) the space of polynomial functions of degree at most $r \geq 1$ on E (resp. the space of polynomial functions of total degree $r \geq 1$ on E). We approximate the pressure and the saturation by discontinuous polynomials of total degrees r_p and r_s respectively.

For any function $q \in \mathcal{D}_r(\mathcal{T}_h)$, we define the jump operator $[[\cdot]]$ and the average operator $\{\cdot\}$ over the interface $e: \forall e \in \Gamma^h$, $[[q]] := q_{E_-} - q_{E_+}$, $\{q\} := \frac{1}{2}q_{E_-} + \frac{1}{2}q_{E_+}$, and $\forall e \in \partial\Omega$, $[[q]] = \{q\} := q_{E_-}$.

In order to treat the strong heterogeneity of the permeability tensor, we follow [8] and introduce a weighted average operator $\{\cdot\}_\omega$:

$$\forall e \in \Gamma^h, \{q\}_\omega = \omega_{E_-} q_{E_-} + \omega_{E_+} q_{E_+} \text{ and } \forall e \in \partial\Omega, \{q\}_\omega = q_{E_-}.$$

The weights are $\omega_{E_-} = \frac{\delta_K^{E_+}}{\delta_K^{E_+} + \delta_K^{E_-}}$, $\omega_{E_+} = \frac{\delta_K^{E_-}}{\delta_K^{E_+} + \delta_K^{E_-}}$ with $\delta_K^{E_-} = n_e^T K_{E_-} n_e$ and $\delta_K^{E_+} = n_e^T K_{E_+} n_e$. Here, K_{E_-} and K_{E_+} are the permeability tensors for the elements E_- and E_+ .

3.1 Semi Discretization in Space

The derivation of the semi-discrete DG formulation is standard (see [11]). First, we multiply each equation of (2) by a test function and integrate over each element, then we apply Green formula to obtain the semi-discrete weak DG formulation. Hence, the aforementioned formulation consists in finding the continuous in time approximations $p_{w,h}(\cdot, t) \in \mathcal{D}_{r_p}(\mathcal{T}_h)$, $s_{n,h}(\cdot, t) \in \mathcal{D}_{r_s}(\mathcal{T}_h)$ such that:

$$\begin{aligned} \mathcal{B}_h(p_{w,h}, \varphi; s_{n,h}) &= l_h(\varphi) \quad \forall \varphi \in \mathcal{D}_{r_p}(\mathcal{T}_h), \forall t \in \mathcal{I}, \\ (\Phi \partial_t s_{n,h}, \psi) + c_h(p_{w,h}, \psi; s_{n,h}) + d_h(s_{n,h}, \psi) &= r_h(\psi) \quad \forall \psi \in \mathcal{D}_{r_s}(\mathcal{T}_h), \forall t \in \mathcal{I}. \end{aligned} \quad (3)$$

The bilinear form \mathcal{B}_h in the total fluid conservation equation of the system (3) is:

$$\mathcal{B}_h(p_{w,h}, \varphi; s_{n,h}) = \mathcal{B}_{bulk,h} + \mathcal{B}_{cons,h} + \mathcal{B}_{sym,h} + \mathcal{B}_{stab,h}. \quad (4)$$

The first term $\mathcal{B}_{bulk,h} := \mathcal{B}_{bulk,h}(p_{w,h}, \varphi; s_{n,h})$ of (4) is the volume term:

$$\mathcal{B}_{bulk,h} = \sum_{E \in \mathcal{T}_h} \int_E (\lambda_t K \nabla p_{w,h} + \lambda_n K \nabla p_{c,h}) \cdot \nabla \varphi - \sum_{E \in \mathcal{T}_h} (\rho_n \lambda_n + \rho_w \lambda_w) K g \cdot \nabla \varphi. \quad (5)$$

The second term $\mathcal{B}_{cons,h} := \mathcal{B}_{cons,h}(p_{w,h}, \varphi; s_{n,h})$, is the consistency term:

$$\begin{aligned} \mathcal{B}_{cons,h} &= - \sum_{e \in \Gamma^h \cup \Gamma_D^h} \int_e \{\lambda_t K \nabla p_{w,h}\}_\omega \cdot n_e [[\varphi]] - \sum_{e \in \Gamma^h \cup \Gamma_D^h} \int_e \{\lambda_n K \nabla p_{c,h}\}_\omega \cdot n_e [[\varphi]] \\ &+ \sum_{e \in \Gamma^h \cup \Gamma_D^h} \int_e \{(\rho_n \lambda_n + \rho_w \lambda_w) K g\}_\omega \cdot n_e [[\varphi]]. \end{aligned} \quad (6)$$

The term $\mathcal{B}_{sym,h} := \mathcal{B}_{sym,h}(p_{w,h}, \varphi; s_{n,h})$, is the symmetry term. Depending on the choice of ε we get different DG methods ($\varepsilon = -1$ SIPG, $\varepsilon = 1$ NIPG, $\varepsilon = 0$ IIPG):

$$\mathcal{B}_{sym,h} = \varepsilon \sum_{e \in \Gamma^h \cup \Gamma_D^h} \int_e \{\lambda_t K \nabla \varphi\}_\omega \llbracket p_{w,h} \rrbracket + \varepsilon \sum_{e \in \Gamma^h \cup \Gamma_D^h} \int_e \{\lambda_n K \nabla \varphi\}_\omega \llbracket s_{n,h} \rrbracket. \quad (7)$$

$\mathcal{B}_{stab,h} := \mathcal{B}_{stab,h}(p_{w,h}, \varphi) = \sum_{e \in \Gamma^h \cup \Gamma_D^h} \gamma_e^p \int_e \llbracket p_{w,h} \rrbracket \llbracket \varphi \rrbracket$ is the stability term.

Following [3], the penalty formulation is: $\gamma_e^p = \sigma_p \frac{r_p(r_p+d-1)|e|}{\min(|E_-|, |E_+|)}$, $\sigma_p \geq 0$.

The right hand side of the total fluid conservation equation of the system (3) is a linear form including the boundary conditions and the source terms.

$$\begin{aligned} l_h(\varphi) = & \int_\Omega (q_w + q_n) \varphi - \sum_{e \in \Gamma_N} \int_e J_t \varphi + \varepsilon \sum_{e \in \Gamma^h} \int_e \lambda_t K \nabla \varphi \cdot n_e p_D \\ & + \varepsilon \sum_{e \in \Gamma_D^h} \int_e \lambda_n K \nabla \varphi \cdot n_e s_D + \sum_{e \in \Gamma_D^h} \gamma_e^p \int_e p_D \varphi, \quad \forall \varphi \in \mathcal{D}_{r_p}(\mathcal{T}_h). \end{aligned} \quad (8)$$

The second equation of the system (3) is the discrete weak formulation of the nonwetting-phase conservation equation where the convection term $-\nabla \cdot (\lambda_n K (\nabla p_w - \rho_n g))$ might be approximated by an upwind discretization technique.

$$\begin{aligned} c_h(p_{w,h}, \psi; s_{n,h}) = & \sum_{E \in \mathcal{T}_h} \int_E (K \lambda_n (\nabla p_{w,h} - \rho_n g)) \cdot \nabla \psi - \sum_{e \in \Gamma^h \cup \Gamma_D^h} \int_e \{K \lambda_n^\# \nabla p_{w,h}\}_\omega \llbracket \psi \rrbracket \\ & + \sum_{e \in \Gamma^h \cup \Gamma_D^h} \int_e \{\rho_n K \lambda_n^\# g\}_\omega \llbracket \psi \rrbracket + \varepsilon \sum_{e \in \Gamma^h \cup \Gamma_D^h} \int_e \{K \lambda_n^\# \nabla \psi\}_\omega \llbracket p_{w,h} \rrbracket, \end{aligned} \quad (9)$$

where $\lambda_n^\# = (1 - \rho) \lambda_{n,E} + \rho \lambda_n^\uparrow$ and λ_n^\uparrow is the upwind mobility:

$$\forall e \in \partial E_- \cap \partial E_+, \quad \lambda_n^\uparrow = \begin{cases} \lambda_{n,E_-} & \text{if } -K(\nabla p_w + \nabla p_c - \rho_n g) \cdot n \geq 0, \\ \lambda_{n,E_+} & \text{else.} \end{cases}$$

Hence depending on the value of $\rho \in \{0, 1\}$, we might use central differencing or upwinding of the mobility for internal interfaces.

The diffusion term $-\nabla \cdot (\lambda_n K \nabla p_c)$ is discretized by a bilinear form similar to that of (4). A more detailed expression can be found in [10].

3.2 Fully Coupled/Fully Implicit DG Scheme

The time interval $[0, T]$ is divided into N intervals $\Delta t_i = t_{i+1} - t_i$ as $0 = t_0 \leq t_1 \leq \dots \leq t_{N-1} \leq t_N = T$. Let p_w^i and s_n^i be the numerical solutions at time t^i . The approximation $s_{n,h}^0$ is chosen as the L^2 projection of the saturation $s_n(0)$. For the

sake of simplicity and easier reading, we apply a first order Adams-Moulton time discretization and Interior Penalty DG for space discretization to the semi-discrete system (3):

$$\begin{aligned}
 \mathcal{B}_h(p_{w,h}^{i+1}, \varphi; s_{n,h}^{i+1}) &= l_h(\varphi), & \forall \varphi \in \mathcal{D}_{r_p}(\mathcal{T}_h), \\
 (\Phi \frac{s_{n,h}^{i+1} - s_{n,h}^i}{\Delta t}, \psi) + c_h(p_{w,h}^{i+1}, \psi; s_{n,h}^{i+1}) + d_h(s_{n,h}^{i+1}, \psi) &= r_h(\psi), & \forall \psi \in \mathcal{D}_{r_s}(\mathcal{T}_h), \\
 (s_{n,h}^0, \zeta) &= (s_n^0, \zeta), & \forall \zeta \in \mathcal{D}_{r_s}(\mathcal{T}_h).
 \end{aligned}
 \tag{10}$$

4 Adaptivity

The first approach considered, *GradIndicator*, is based on a heuristic indicator which depends on the local gradient of the DG solution measured in the L^2 norm. We define on each element E of the mesh, the indicator η_E^i at time step i , such that: $\eta_E^i = \|\nabla s_n^i\|_{L^2(E)}$, $\forall E \in \mathcal{T}_h$. Each element whose indicator η_E^i is greater than a threshold value $\eta_{Tol} \geq 0$ is refined.

For the second approach, the choice between h -adaptivity and p -adaptivity depends heavily on the value of a smoothness indicator ς_E . Given an error indicator η_E , $E \in \mathcal{T}_h$, we define η_E^{r-1} the L^2 projection into a lower order polynomial space $\mathcal{D}_{r-1}(\mathcal{T}_h)$. The derivation of this L^2 projection is quite straightforward due to the hierarchical aspect of the modal DG bases implemented. The indicator $\eta_E = \|s_n\|_{H^1(E)}$ allows to refine the mesh when the solution is estimated to be rough and increase the polynomial degree when the solution is estimated to be smooth. The use of heuristic error indicators requires a maximum level of allowed h -refinement *maxlevel* to be specified to avoid overly aggressive refinement. Whenever an element is selected for h -refinement it is also selected for p -coarsening in order to reduce the oscillations in the vicinity of the front of the propagation. An hp -adaptive strategy of this type called *PRIOR2P* as in [12] is implemented. In that approach, the smoothness indicator is $\varsigma_E \sim 1 - \frac{\log((\eta_E^{r-1})/(\eta_E^{r-2}))}{\log((r-1)/(r-2))}$, where r is the local polynomial degree.

5 Numerical Simulations

In this section we present some numerical tests for the adaptive DG scheme. All test cases are implemented with the Interior Penalty methods. In order to ensure second order accuracy, we employ a central differencing of the mobility for internal interfaces thus following a similar approach to that of Rivière et al. [7].

5.1 2d Flow Problem

We consider here a two dimensional test case that admits an exact solution from [2] aiming to examine the L^2 error of the DG methods. The problem depicts the transport of a Gaussian pulse in a rotating flow field. Considering $\Omega = (-0.5, 0.5)^2$ and $J = (0, T)$, we search for (S) such that: $\frac{\partial S}{\partial t} + \nabla \cdot (uS + K\nabla S) = 0$ in $\Omega \times J$.

The problem boundary and initials conditions derive from the exact solution $S(x, y, t) = 2\sigma^2 / (2\sigma^2 + 4Kt) e^{(-\frac{(\bar{x}-x_c)^2 + (\bar{y}-y_c)^2}{2\sigma^2 + 4Kt})}$ where, $u = (-4y, 4x)^T$, $\bar{x} = x\cos(4t) + y\sin(4t)$, $\bar{y} = -x\sin(4t) + y\cos(4t)$, $x_c = -0.25$, $y_c = 0$, $K = 10^{-4}$ and $2\sigma^2 = 0.004$.

The domain is subdivided uniformly into square elements. The coarsest mesh consist of 8×8 elements. The solutions are approximated by piecewise polynomials of order k , $k \in \{1, 2, 3, 4\}$. The penalty parameter $\sigma_p = 10^{-10}$. Figures 1, 2 and 3 provide contours of the solution for the IIPG scheme combined with second order Adams-Moulton method time discretization. The numerical analysis in Table 1 shows that the PRIOR2P indicator yields a smaller L^2 error.

5.2 3d Heterogeneous Problem

In this section, we focus on a three-dimensional case. We also consider different sand types with different permeabilities and different entry pressures (Table 2).

The bottom of the reservoir is impermeable for both phases. Hydrostatic conditions for the pressure p_w and homogeneous Dirichlet conditions for the saturation s_n are prescribed at the lateral boundaries. A flux of $0.25 \text{ Kg s}^{-1}\text{m}^{-2}$ of

Fig. 1 Rotating pulse, solution at T=0.4

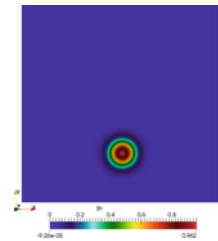


Table 1 L^2 error for solution at $T = 0.4$

| | $\ S - S_h\ _{L^2(\Omega)}$ | Final nb of DOFs | Avg nb of lin it/ Newton cycle | Avg inv time/ Newton [s] | Avg assem time / Newton [s] |
|---------------|-----------------------------|------------------|--------------------------------|--------------------------|-----------------------------|
| GradIndicator | 3.06×10^{-04} | 19230 | 28.63 | 0.0525 | 0.44 |
| PRIOR2P | 3.494×10^{-06} | 46750 | 33.36 | 0.096 | 0.96 |

the DNAPL is infiltrated from the top into a domain of depth of 1 m. The initial ALUCubeGrid mesh consist of $17 \times 17 \times 17$ hexahedral elements and resolves the interfaces between regions with different permeabilities. 150 time steps of length $\Delta t = 20$ s are computed (final time $T = 3000$ s). This grid is locally adapted (non-conforming). We also set $r_p = r_s$ for the problem.

Figure 4 illustrates the evolution of the nonwetting saturation during the simulation. The effects of the *hp* algorithm are reflected in the mesh distribution showing an intense refinement and lower polynomial degree in the parts of the domain where the value of the indicator is above the threshold value. The second row of Fig. 4 shows the drastic improvement of the front shape and the reduction of the oscillations in the vicinity of the front when *h* and *hp*-adaptive methods are used. Table 3 provides more details concerning the computational effort.

6 Conclusion & Outlook

In this work, we have introduced an adaptive discontinuous Galerkin scheme for incompressible, immiscible two-phase flow in strongly heterogeneous porous media with gravity forces and discontinuous capillary pressures. We considered as a 3*d* test case a DNAPL infiltration in an initially water saturated reservoir. The oscillations appearing in the vicinity of the front of the propagation are reduced with the local

Table 2 3d problem parameters

| | Ω_1 | Ω_2 | $\Omega \setminus \Omega_1 \cap \Omega \setminus \Omega_2$ |
|---------------|------------------------|------------------------|--|
| Φ [-] | 0.39 | 0.39 | 0.40 |
| k [m^2] | 6.64×10^{-16} | 6.64×10^{-15} | 6.64×10^{-11} |
| S_{wr} [-] | 0.1 | 0.1 | 0.12 |
| S_{nr} [-] | 0.00 | 0.00 | 0.00 |
| θ [-] | 2.0 | 2.0 | 2.70 |
| p_d [Pa] | 5000 | 5000 | 755 |

Table 3 L^2 error for solution at $T = 0.4$

| | Final nb of DOFs | Avg nb of lin it/ Newton cycle | Avg inv time/ Newton [s] | Avg assem time / Newton [s] | Total CPU time [s] |
|----------------|------------------|--------------------------------|--------------------------|-----------------------------|--------------------|
| No-adapt deg=2 | 196520 | 96.19 | 2.97 | 33.9 | 7360.3 |
| h-adapt deg=1 | 171232 | 127.157 | 20.38 | 9.86 | 6740.4 |
| h-adapt deg=2 | 398680 | 509.56 | 78.0 | 16.26 | 19812.1 |
| hp-adapt deg2 | 296680 | 468 | 70.69 | 28.3 | 19294.8 |

Fig. 2 Polynomial degrees at $T = 0.4$ for GradIndicator

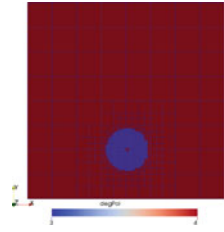


Fig. 3 Polynomial degrees at $T = 0.4$ for PRIOR2P

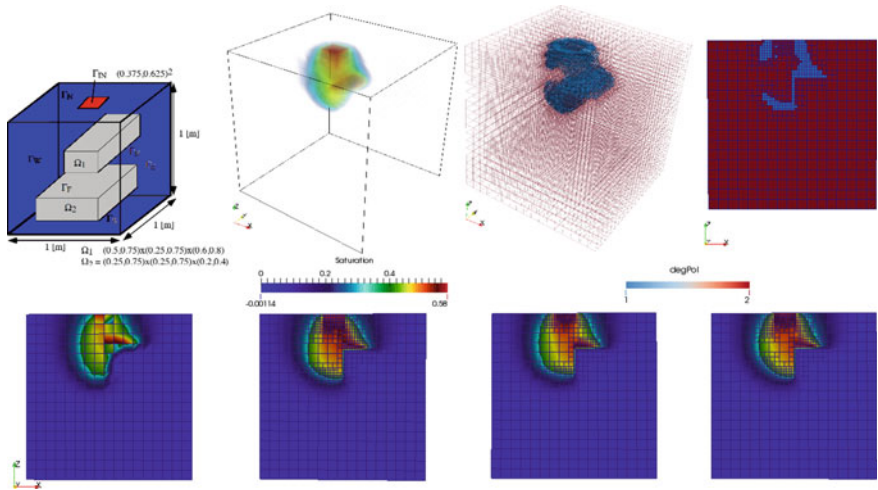
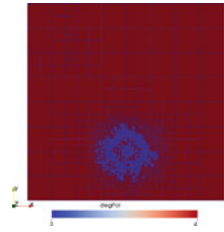


Fig. 4 First row from left to right, domain geometry, contour plot of saturation distribution after 3000 s of injection, mesh distribution, polynomial degree distribution along the slice $y = 0.45$. Second row saturation profile along the slice $y = 0.45$; from left to right, non-adaptive with $r_p = r_s = 2$, h-adaptive with $r_p = r_s = 1$, h-adaptive with $r_p = r_s = 2$, hp-adaptive with $\max\{r_p, r_s\} = 2$

mesh refinement and the decrease of the local polynomial order. Future work will be concerned with the derivation of robust anisotropic *hp*-adaptive methods and the extension to other DG methods such as the Compact Discontinuous Galerkin 2 (CDG2) [4].

Acknowledgements Birane Kane acknowledges the Cluster of Excellence in Simulation Technology (SimTech) at the University of Stuttgart for financial support. Robert Klöfkom acknowledges the Research Council of Norway and the industry partners – ConocoPhillips Skandinavia AS, BP Norge AS, Det Norske Oljeselskap AS, Eni Norge AS, Maersk Oil Norway AS, DONG Energy A/S, Denmark, Statoil Petroleum AS, ENGIE E&P NORGE AS, Lundin Norway AS, Halliburton AS, Schlumberger Norge AS, Wintershall Norge AS – of The National IOR Centre of Norway for financial support.

Both authors would like to thank the reviewers for helpful comments to improve this work.

References

1. Bastian, P.: Numerical computation of multiphase flow in porous media. Ph.D. thesis, habilitationsschrift Univeristät Kiel (1999)
2. Bastian, P.: Higher order discontinuous galerkin methods for flow and transport in porous media. In: Challenges in Scientific Computing-CISC 2002, pp. 1–22. Springer (2003)
3. Bastian, P.: A fully-coupled discontinuous galerkin method for two-phase flow in porous media with discontinuous capillary pressure. *Comput. Geosci.* **18**(5), 779–796 (2014)
4. Brdar, S., Dedner, A., Klöfkom, R.: Compact and stable discontinuous galerkin methods for convection-diffusion problems. *SIAM J. Sci. Comput.* **34**(1), 263–282 (2012)
5. Brooks, R.H., Corey, A.T.: Hydraulic properties of porous media and their relation to drainage design. *Trans. ASAE* **7**(1), 26–0028 (1964)
6. Cancès, C., Pop, I., Vohralík, M.: An a posteriori error estimate for vertex-centered finite volume discretizations of immiscible incompressible two-phase flow. *Math. Comput.* **83**(285), 153–188 (2014)
7. Epshteyn, Y., Rivière, B.: Fully implicit discontinuous finite element methods for two-phase flow. *Appl. Numer. Math.* **57**(4), 383–401 (2007)
8. Ern, A., Mozolevski, I., Schuh, L.: Discontinuous galerkin approximation of two-phase flows in heterogeneous porous media with discontinuous capillary pressures. *Comput. Methods Appl. Mech. Eng.* **199**(23), 1491–1501 (2010)
9. Ern, A., Proft, J.: A posteriori discontinuous galerkin error estimates for transient convection-diffusion equations. *Appl. Math. Lett.* **18**(7), 833–841 (2005)
10. Kane, B.: Using dune-fem for adaptive higher order discontinuous galerkin methods for two-phase flow in porous media. *Arch. Numer. Softw.* (submitted)
11. Klieber, W., Riviere, B.: Adaptive simulations of two-phase flow by discontinuous galerkin methods. *Comput. Methods Appl. Mech. Eng.* **196**(1), 404–419 (2006)
12. Mitchell, W.F., McClain, M.A.: A comparison of *hp*-adaptive strategies for elliptic partial differential equations. *ACM Trans. Math. Softw. (TOMS)* **41**(1), 2 (2014)
13. Vohralík, M., Wheeler, M.F.: A posteriori error estimates, stopping criteria, and adaptivity for two-phase flows. *Comput. Geosci.* **17**(5), 789–812 (2013)